BMC Cancer

RESEARCH

Open Access

A non-invasive nomogram for the prediction of poor prognosis of hepatocellular carcinoma based on the novel marker Interleukin-41

Zihan Mu[3†], Jiaojiao Su[3†], Jiuhua Yi[3], Rui Fan[3], Jiayuan Yin[3], Yazhao Li[2*] and Bowen Yao[1*]

Abstract

Death and tumor recurrence are both important adverse prognostic factors for hepatocellular carcinoma(HCC) patients. This article aims to discuss the risk factors for recurrence and death in patients with HCC after R0 resection, and to establish a nomogram model for predicting the recurrence and death of HCC patients.A total of 224 HCC patients after R0 resection were enrolled and divided into a training cohort ($n=149$) and a validation cohort ($n=75$) The risk factors for recurrence and death were determined based on cox regression analysis. A nomogram containing independent risk predictors was established and validated.The recurrence rate of 224 cases of HCC after R0 resection was 43.30%. The high expression of interleukin-41(IL41) (HR = 2.446, $P=0.000$), intratumoral artery (HR = 1.862, $P=0.005$), and MVI1 subgroup of microvascular invasion(MVI) grade (HR = 1.541, $P=0.031$) are independent risk factors associated with recurrence after resection of HCC. The mortality rate was 15.63%. The high expression of IL-41 (HR = 4.679, $P=0.000$), tumor size ≥ 5 cm (HR = 3.745, $P=0.001$), and Aspartate transaminase(AST) concentration 45-90u/L (HR = 2.837, $P=0.015$) are independent risk factors associated with mortality. Interleukin-41(IL-41), microvascular invasion(MVI), and intratumoral artery are independent risk factors for recurrence after resection of hepatocellular carcinoma. IL-41, tumor size, and Aspartate transaminase(AST) are independent risk factors for death after resection of hepatocellular carcinoma. We developed and validated two multivariate nomograms, and conducted validation. The nomogram models have achieved ideal results in predicting the recurrence and death of HCC patients.

Keywords Hepatocellular carcinoma, Interleukin-41, Nomogram model, Recurrence, Death

Introduction

Hepatocellular carcinoma (HCC) is the sixth most common cancer globally and the second leading cause of cancer deaths in 2022 [1]. In China, hepatectomy is the preferred treatment for Chinese Liver Cancer Stage (CNLC) Ia, Ib, and IIa HCC. For patients with CNLC IIb and IIIa HCC who are eligible for transarterial chemoembolization (TACE) and systemic treatment, respectively, complete resection can be considered if the tumor nodules are located within the same segment [2]. However, early postoperative recurrence and mortality have been major drawbacks of this surgery for the past 20 years.

†Zihan Mu and Jiaojiao Su contributed equally to this work.

*Correspondence:
Yazhao Li
xjtu_lyz@163.com
Bowen Yao
ybwsplendid@xjtufh.edu.cn
[1]Department of Hepatobiliary Surgery, The First Affiliated Hospital of Xi'an Jiaotong University, Xi'an, China
[2]Center for Translational Medicine, The First Affiliated Hospital of Xi'an Jiaotong University, Xi'an, China
[3]Zonglian College, Xi'an Jiaotong University Health Science Center, Xi'an, China

HCC recurs in 20-40% of patients within 1 year after hepatectomy, in more than 50% of patients with early-stage HCC (such as CNLC Ia, Ib, and IIa) at 5 years after hepatectomy, and in approximately 70-80% of patients with intermediate or advanced HCC on an annual basis [3]. Furthermore, the 1-year HCC mortality rate is 9.7%. Improved diagnostic procedures, surgical techniques, and perioperative management are essential for enhancing the outcomes of hepatectomy [4]. Therefore, there is an urgent need to identify effective predictors of early recurrence and mortality following hepatectomy in HCC patients.

Previous studies have shown that early recurrence is often associated with pathological characteristics of invasive tumors, such as large tumor size, multiple tumors, poor differentiation, microvascular invasion (MVI), satellite nodules, and tumor capsular invasion. Additionally, advanced tumor stage, preoperative carcinoembryonic antigen (CEA) levels, portal vein tumor thrombus (PVTT), non-alcoholic fatty liver disease, active hepatitis, and elevated alpha-fetoprotein (AFP) levels contribute to early recurrence [5–10]. On the other hand, late HCC recurrence was reported to be primarily linked to underlying liver diseases, such as cirrhosis and active hepatitis. It is important to note that while most of these studies have explored factors associated with an increased risk of tumor recurrence, they have not developed multivariable prediction models that integrate these risk factors. Current models for predicting poor prognosis after hepatectomy are predominantly based on intraoperative factors, radiomics, and biochemical markers, including deep learning and machine learning models. However, these models are limited by significant data heterogeneity and the need for invasive surgery [11–14].

The risk factors for mortality following hepatectomy in HCC patients remain poorly understood. The presence of multiple tumors, liver Cirrhosis, vascular invasion, elevated serum AFP levels, and large tumor size have been identified as potential risk factors for early HCC mortality [4, 15–17]. Currently, studies have developed risk prediction models for adverse prognosis in hepatocellular carcinoma (HCC) patients based on pathological features (Such as vascular and hepatic plate structural characteristics), molecular mechanisms (Such as disulfidptosis), and inflammatory markers (Such as neutrophil-to-lymphocyte ratio [NLR], platelet-to-lymphocyte ratio [PLR], and C-type natriuretic peptide [CNP]) [18–20]. Other studies have incorporated sarcopenia as a key factor into nomogram models for predicting poor prognosis in HCC [21]. Although these models comprehensively integrate patient physiological status, perioperative outcomes, and tumor characteristics, limitations persist, including complex data measurement protocols, applicability restricted to postoperative decision-making, and reliance on single-center cohorts. Hence, there is an urgent need for a novel prognostic marker for HCC. Previous research has identified multiple biomarkers predictive of adverse HCC prognosis, such as interleukin-6 (IL-6), des-γ-carboxy prothrombin (DCP), and α-fetoprotein-L3 (AFP-L3). These markers elucidate molecular mechanisms underlying poor prognosis through pathways involving the inflammatory microenvironment, angiogenesis, and cancer stem cells, respectively [22, 23]. A previous work of this research group showed that interleukin-41 (IL-41) is elevated in the serum of HCC patients and is closely associated with poor prognosis [24]. AFP is a widely used biomarker for HCC [25–27].However, the proprotion of AFP-negative HCC patients(We use 20ng/ml as the threshold to distinguish between AFP-positive and AFP-negative) has increased in recent years due to the effective treatment and control of hepatitis [28–30]. In our prior investigations, we observed an inverse correlation between IL-41 expression levels and AFP concentrations in AFP-negative HCC patients. Elevated IL-41 expression was associated with poorly differentiated tumors, AFP positivity, unfavorable prognosis, and post-resection recurrence. Notably, serum IL-41 levels were significantly lower in patients with late recurrence (≥ 2 years post-resection) compared to those with early recurrence or mortality, further underscoring IL-41's prognostic value in predicting adverse HCC outcomes.In this study, a prediction model incorporating IL-41 as a primary risk factor was constructed and validated to be effective for predicting post-hepatectomy recurrence and death in HCC.

Methods

Study population and collection of clinicopathological and imaging data

The selection of the study population and the study design are illustrated in Fig. 1. Patients diagnosed with HCC who underwent hepatectomy at the First Affiliated Hospital of Xi'an Jiaotong University between August 2015 and July 2022 were screened based on the eligibility criteria. Inclusion criteria: (1) HCC patients with accurate pathological diagnosis (2) HCC patients undergo radical liver cancer resection and have not received any anti-tumor treatment before or after surgery, such as transarterial chemoembolization (TACE), radiofrequency ablation, and anti-tumor drugs (3) HCC patients with complete clinical pathology, laboratory, imaging, and follow-up data (with a follow-up time of at least 2 years in our center). Exclusion criteria: (1)Perioperative death; (2)Presence of other malignancies in the patient's medical history; (3) Unexpected deaths during follow-up (such as COVID-19 or car accidents); (4) Postoperative loss to follow-up. A total of 224 patients were ultimately included in this study. The participants were randomly

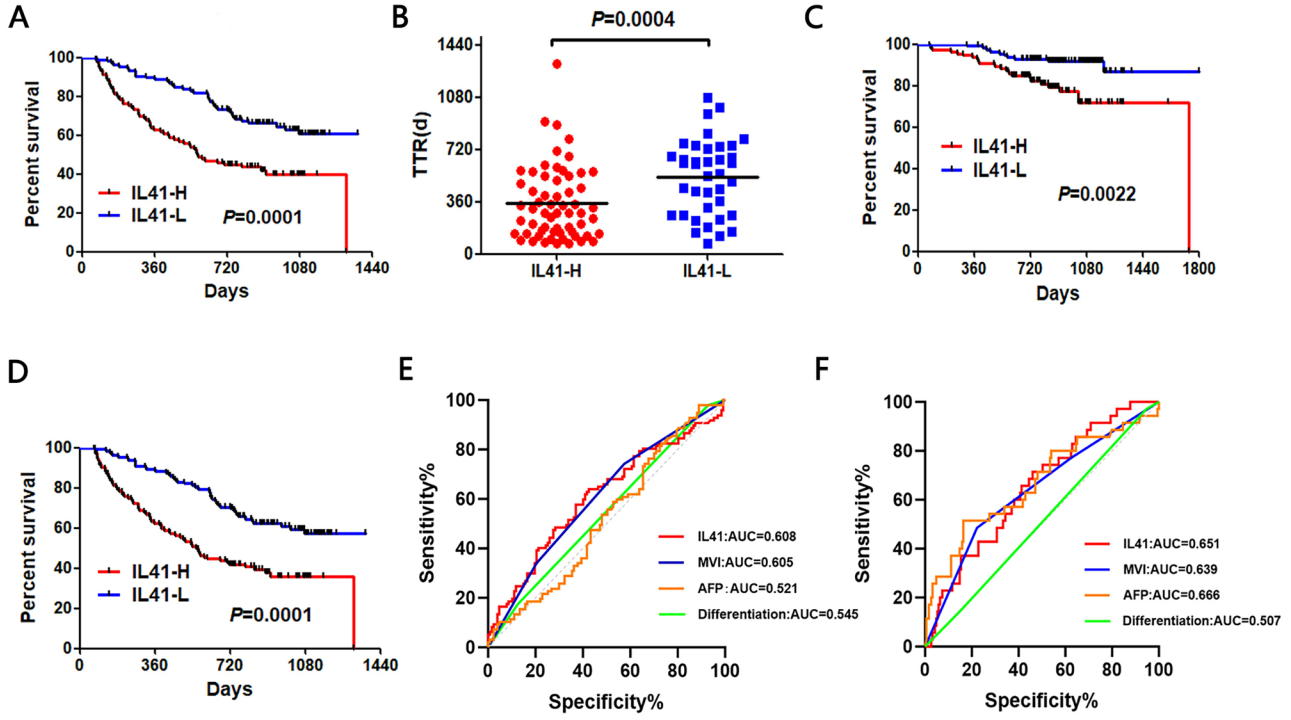

Fig. 1 Prediction of poor prognosis of liver cancer by IL41. **(A)**RFS of all HCC patients associated with high and low expression of IL41 (*P=0.0001). **(B)** TTR of all HCC patients associated with high and low expression of IL41 (*P=0.0004). **(C)** OS of all HCC patients associated with high and low expression of IL41 (*P=0.0022). **(D)** PFS of all HCC patients associated with high and low expression of IL41 (*P=0.0001). **(E)** ROC curves for predicting recurrence in HCC patients using IL41, MVI, AFP, and differentiation degree. **(F)** ROC curves for predicting death in HCC patients using IL41, MVI, AFP, and differentiation degree.OS: overall survival; RFS: recurrence-free survival; PFS: progression-free survival; TTR: time to disease recurrence

assigned 2:1 to the training cohort (n=150) or the validation cohort (n=74). A prediction model was constructed using the training set and its performance was assessed using the validation set. This retrospective study was approved by the Ethics Committee of the First Affiliated Hospital of Xi'an Jiaotong University. All patients who underwent serological testing (such as IL-41) and had pathology and histology results for post-hepatectomy samples have given informed consent.

Data collected included demographics (such as age and gender), preoperative hematology, serum chemistry and tumor marker results (such as AFP, hepatitis B virus (HBV), hepatitis C virus (HCV), Aspartate transaminase(AST), alanine transaminase (ALT), bilirubin, albumin, neutrophil count, platelet counts, and lymphocyte count), pathological features of the tumor (such as tumor size, degree of tumor and surgical margins), and preoperative contrast-enhanced computed tomography (CT) findings (such as intrathoracic necrosis, peritumoral hemorrhage, peritumoral enhancement, tumor shape, and intratumoral arteries) (see Fig. 2).

Follow-up

All patients were regularly followed up after hepatectomy in accordance with clinical guidelines. Recurrent HCC was diagnosed based on two or more investigations, including ultrasound, contrast-enhanced CT, magnetic resonance imaging (MRI), and hepatic arteriography with or without elevated serum AFP levels. HCC-related deaths were confirmed by obtaining relevant information from the hospital follow-up clinic. The last follow-up date was March 31, 2024 for patients without evidence of recurrence (see Fig. 3).

ELISA

Serum samples were collected from all enrolled patients prior to hepatectomy and immediately stored at -80 °C until use. The serum concentrations of human IL-41 were determined using the Human Interleukin-41 (IL-41) Quantification Kit (RX100486) according to methods described previously [24]. In brief, a high-affinity microtiter plate was coated with anti-human IL-41 monoclonal antibody, incubated with diluted serum samples (1:5) and standards, washed, incubated with biotinylated anti-hIL-41 detection antibody, washed, incubated with horseradish peroxidase-labeled streptavidin (Streptavidin-HRP), washed, and incubated with the chromogenic substrate TMB. The reaction was terminated by the addition of a termination solution, and absorbance at 450 nm was measured using a microplate meter. A standard curve was constructed by plotting the concentrations of the standards on the x-axis (six standards plus

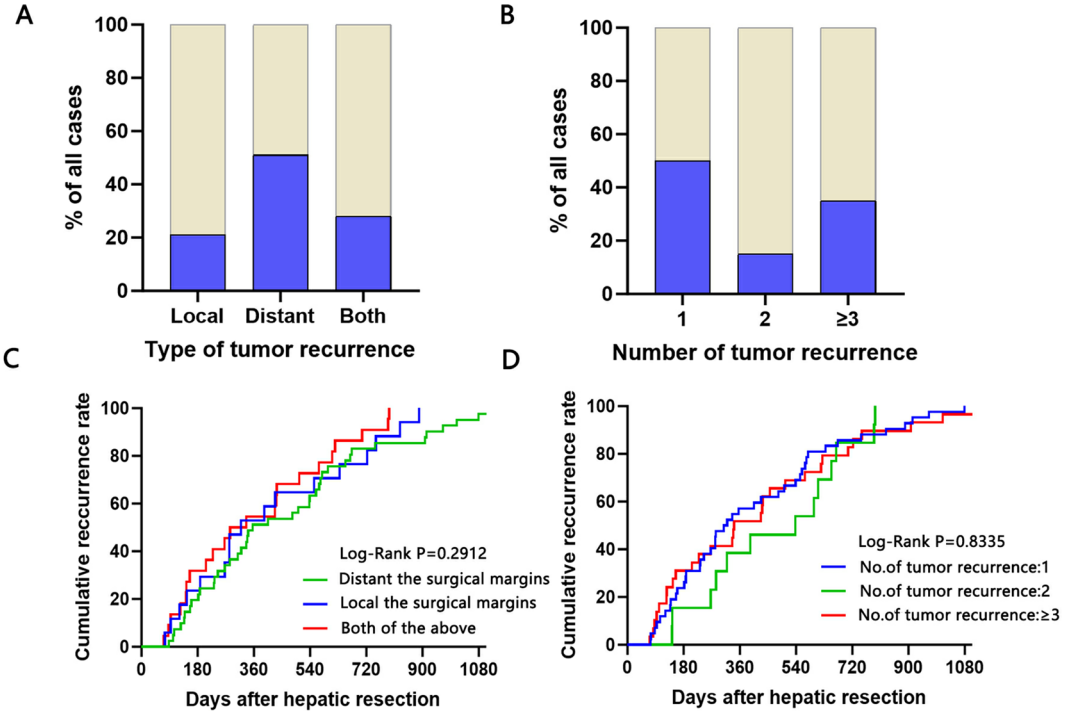

Fig. 2 Recurrence patterns and differences between groups in TTR. **(A)** The pattern of recurrence according to the type of recurrent tumors. **(B)** The pattern of recurrence according to the number of recurrent tumors. **(C)** Group differences in time to the type of recurrence were examined with the log-rank test(**P* = 0.2912). **(D)** Group differences in time to the number of recurrence were examined with the log-rank test(**P* = 0.8335). TTR: time to recurrence

one blank, totaling seven concentration points) and their corresponding optical density (OD) values on the y-axis, followed by four-parameter logistic curve fitting. Serum IL-41 concentrations in the test samples were determined from their OD values using the standard curve (see Fig. 4).

Statistical analysis and nomogram development

Statistical analyses were conducted using IBM SPSS 25.0 and R 4.4.1. Nomograms and receiver operating characteristic (ROC) curves were generated using RStudio. Continuous variables are expressed as mean ± standard deviation (SD) and compared using the independent samples *t*-test. Categorical variables are analyzed using the Chi-square test or Fisher's exact test. The 3-year recurrence-free survival (RFS) was calculated using the Kaplan-Meier estimator and compared between groups using the log-rank test. Univariate and multivariate Cox proportional hazard regressions were performed to identify independent risk factors for HCC recurrence or death. Perform multivariate Cox analysis using variables that have reached statistical significance in univariate Cox analysis, and incorporate variables that have reached statistical significance in multivariate Cox analysis into the nomogram model.All statistical tests were two-tailed, and a $P < 0.05$ was considered statistically significant (see Fig. 5).

A nomogram was developed based on the identified risk factors to predict the 12- and 36-month RFS.Convert each regression coefficient in multivariate Cox proportional hazards regression proportionally to a 0-100 point scale, and assign 100 points to the effect of the variable with the highest beta coefficient (absolute value). And established column charts for predicting 1-year and 3-year RFS. The total score is obtained by adding the scores of each independent variable, and the total score is converted into the predicted probability. The cutoff value for IL-41 was determined by ROC curve analysis and used to stratify patients into the high-expression and low-expression subgroups. The predictive performance of the nomogram was evaluated and compared between the training and validation cohorts using the ROC curves. The clinical utility of the nomogram in the training and validation cohorts was assessed by the clinical impact curve (CIC) and decision curve analysis (DCA) in RStudio (see Fig. 6).

Results

Baseline characteristics of the training and validation cohorts

A total of 224 patients with confirmed HCC who received treatment at this hospital between 2015 and 2022 were included in this study. These patients had well-preserved serological and pathological tissue samples, had not been lost to follow-up for more than 2 years, and underwent

A

	β coefficient	SE	Wald	HR（95%CI）	P value	Points assigned
MVI grade：M1	0.365	0.331	1.219	1.441（0.753,2.755）	0.270	27.218
MVI grade：M2	1.341	0.340	15.566	3.824（1.964,7.445）	0.000	100
Intratumoral artery	0.315	0.292	1.161	1.370（0.773,2.427）	0.281	23.490
IL41-H	0.852	0.260	10.735	2.345（1.409,3.906）	0.001	63.535

B

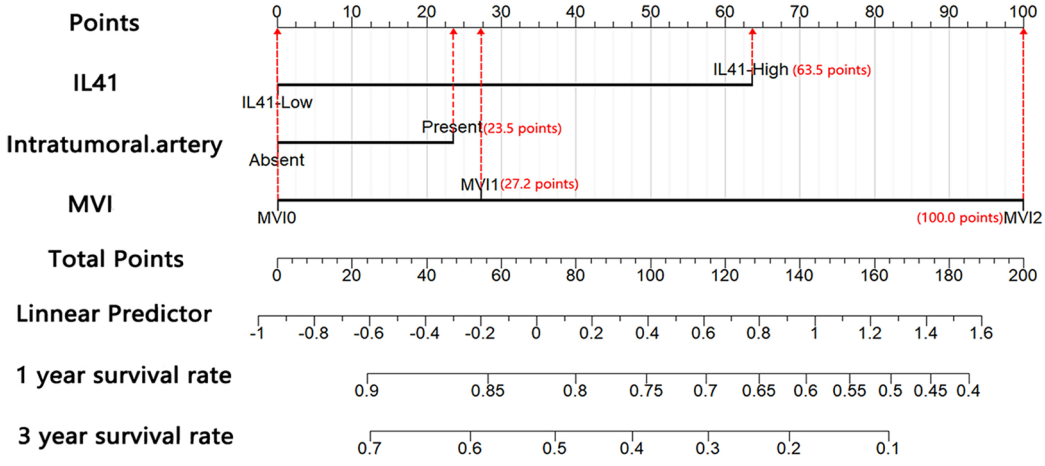

C

	β coefficient	SE	Wald	HR（95%CI）	P value	Points assigned
AST:＞90pg/ml	1.428	0.786	3.299	4.170（0.893,19.467）	0.069	81.275
AST:40-90pg/ml	1.514	0.503	9.064	4.545（1.696,12.180）	0.003	86.170
Tumor size:＞5cm	1.757	0.506	12.040	5.793（2.148,15.628）	0.001	100
IL41-H	1.213	0.487	6.206	3.365（1.295,8.740）	0.013	69.038

D

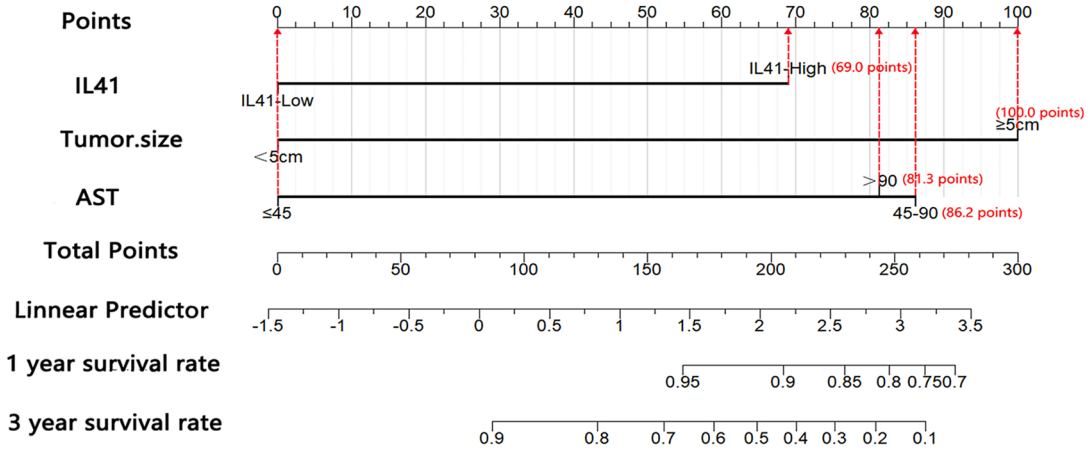

Fig. 3 Development of the nomogram model for predicting recurrence. **(A)** The points assignments of variables based on Cox regression analysis. **(B)** Nomogram model depicting 12 – and 36 – month RFS. **(C)** The points assignments of variables based on Cox regression analysis. **(D)** Nomogram model depicting 12 – and 36 – month PFS. The use of nomogram was as follows: Points are assigned for each variable by drawing a straight line upward from the corresponding value to the "Points" line. Then, sum the points received for each variable, and locate the number on the "Total Points" axis. The 12 – and 36 – month RFS/PFS can be calculated by connecting each point to the survival line. IL41,interleukin-41;MVI, microvascular invasion, RFS, recurrence – free survival. AST, aspartate transaminase, PFS, recurrence – free survival

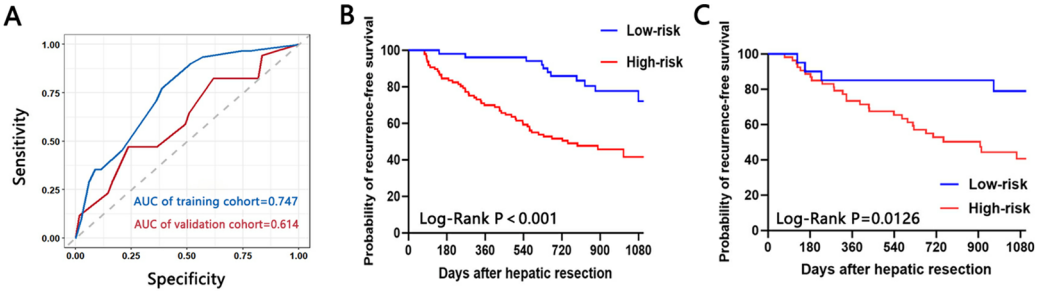

D

Months after Hepatic resection	0	6	12	18	24
No.of patients at risk					
Low-risk	52	51	49	47	39
High-risk	95	80	65	53	44

E

Months after Hepatic resection	0	6	12	18	24
No.of patients at risk					
Low-risk	17	16	15	15	15
High-risk	56	47	38	32	24

Fig. 4 Validation of the nomogram model for predicting recurrence. **(A)** The ROC curve and AUC with 95% CI in the training cohort and validation cohort. Kaplan–Meier survival analysis of the high-risk, middle-risk, and low-risk HCC patients in the training cohort **(B)** and validation cohort **(C)**. The recurrence status of of high-risk, medium risk, and low-risk HCC patients in the training cohort **(D)** and validation cohort **(E)**. ROC, Receiver Operating Characteristic; AUC, Area Under Curve; CI, confidence interval

radical hepatectomy for HCC for the first time. The study population comprised of 174 males and 50 females with a mean age of 56.9 years (range: 25–81 years). Based on the follow-up data and diagnostic criteria, 97 patients (43.3%) experienced tumor recurrence, while 127 patients (56.7%) exhibited no evidence of recurrence at the final follow-up. Additionally, 35 patients (15.6%) died, while 189 patients (84.4%) demonstrated no evidence of mortality at the final follow-up. There were no significant differences in baseline characteristics between the training and validation cohorts (Table 1).

IL-41 is a predictor for HCC progression and poor prognosis

IL-41 was identified as a serologic and histologic marker for HCC and a valuable predictor for disease progression and poor prognosis especially in AFP-negative patients. In this study, patient sample size was expanded and follow-up data were collected over a period of two years. By plotting the ROC curve and calculating the Youden's index, we determined the cutoff value for grouping the IL41 high-expression group and IL41 low-expression group to be 78.05 pg/mL(When using this cutoff value, the sensitivity for predicting recurrence was 61.9%, and the specificity was 58.3%; the sensitivity for predicting death was 71.4%, and the specificity was 53.4%).The present analysis revealed that the IL-41 high-expression group had significantly lower postoperative RFS ($P = 0.0001$, Fig.S1A) and earlier postoperative recurrence (TTR) ($P = 0.0004$, Fig.S1B) than the IL-41 low-expression group. Similarly, the IL-41 high-expression group also exhibited markedly shorter overall survival (OS) ($P = 0.0022$, Fig.S1C) and progression-free survival (PFS; $P = 0.0001$, Fig.S1D) compared to the IL-41 low-expression group. These data demonstrate that high IL-41 expression is closely associated with poor prognosis in HCC following hepatectomy.

In our previous research, we found that serum IL-41 expression was significantly correlated with microvascular infiltration (MVI), poorly differentiated cancer cells, and preoperative high AFP, which can predict poor prognosis of HCC. To determine the predictive ability of IL-41, AFP, MVI, and differentiation degree for poor prognosis, we plotted ROC curves for predicting recurrence and death after HCC resection. In the ROC curves for predicting recurrence after HCC resection, the areas under the ROC curves for IL-41, AFP, MVI, and differentiation degree were 0.608 (95% confidence interval [CI]: 0.532–0.684), 0.521 (95% CI: 0.445–0.597), and 0.606 (95% CI: 0.531-0.6), respectively. 80) and 0.545 (95% CI: 0.469–0.621) (Fig.S1E). The results indicate that IL-41 has a good predictive ability for HCC recurrence, and the ability of IL-41 to predict HCC recurrence

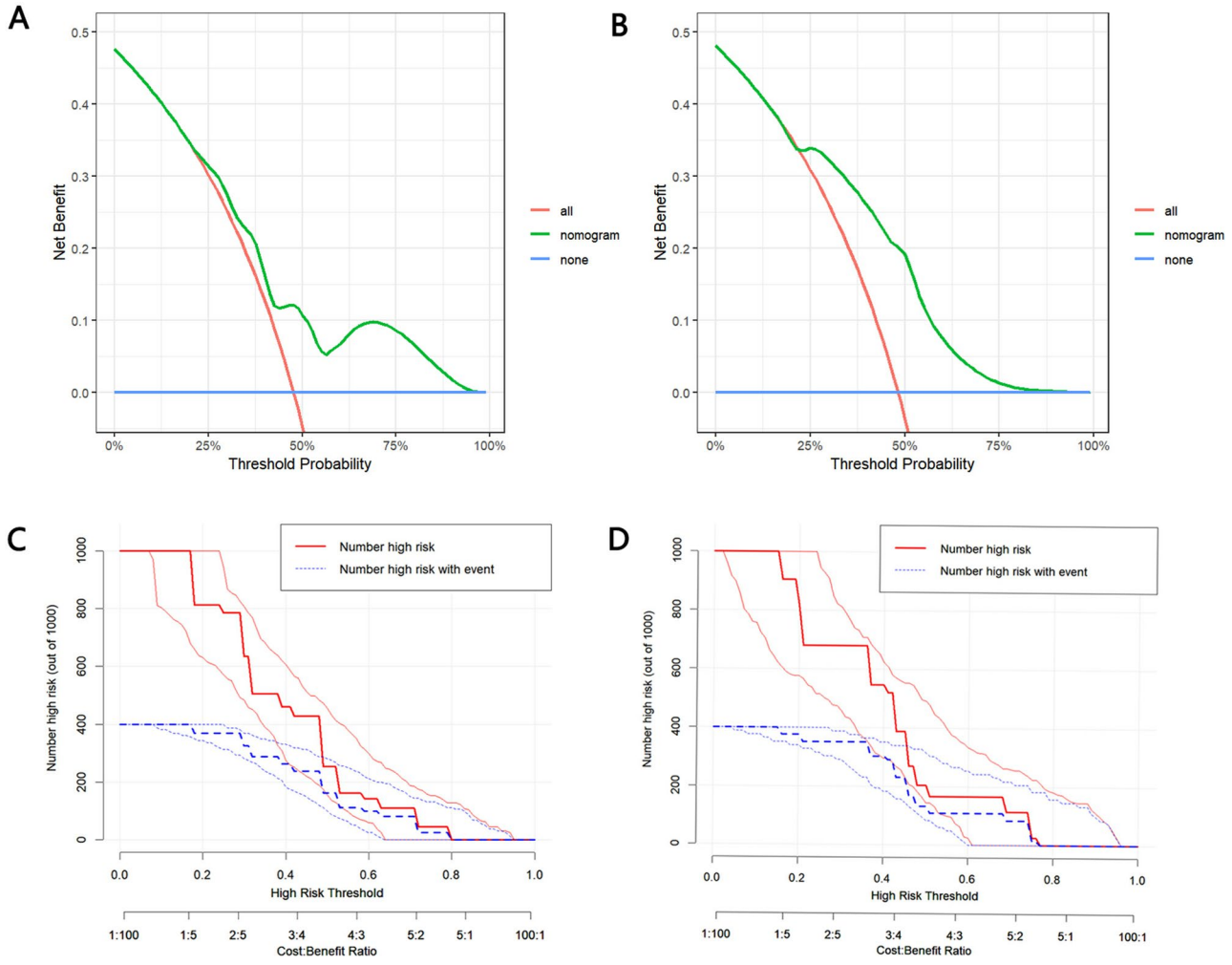

Fig. 5 DCA of column charts in training and validation cohort **(A**, **B)**. The Y-axis displays net benefits. The X-axis represents the threshold probability. None-line (blue line) represents the net benefit when no participants are considered with recurrence. All- line (red line) represents the net benefit when all participants are considered with recurrence. The green line represents the net benefit of the nomogram at different threshold probabilities. The area between the "none-line" (blue line) and "all- line" (red line) in the model curve represents the clinical practicality of the model. CIC used to predict the presence of recurrent column charts in the training cohort **(C)** and validation cohort **(D)**. Under different threshold probabilities in a given population, the number of high-risk patients and the number of high-risk patients with recurrence are displayed.;DCA, Decision Curve Analysis; CIC, Clinical impact curve

is higher than AFP, MVI, and differentiation degree in these patient data. The areas under the ROC curves for IL-41, AFP, MVI, and differentiation degree in predicting postoperative death after HCC resection were 0.651 (95% CI: 0.557–0.745), 0.668 (95% CI: 0.560–0.777), 0.639 (95% CI: 0.535–0.744), and 0.508 (95% CI: 0.406–0.610), respectively (Fig.S1F). The results indicate that IL-41 also has a good predictive ability for postoperative mortality after HCC resection.

Patterns of HCC recurrence

Recurrence patterns were assessed in three ways: (1) type of recurrent tumor: local recurrence at the surgical margin (recurrent tumor within 20 mm of the surgical margin), distant intrahepatic recurrence (recurrent tumor more than 20 mm from the surgical margin), or both; (2) number of recurrent tumors: single, 2, or ≥ 3; and (3) TTR. Among the 97 patients who experienced tumor recurrence, 17 patients were excluded due to the inability to determine the recurrent tumor type. Of the remaining 80 patients, 41 (51.25%) had recurrent tumors distal to the surgical margins, 17 (21.25%) had recurrent tumors within 20 mm of the surgical margins, 22 (27.50%) had both distal and proximal recurrences (Fig.S2A). Excluding the 10 patients for whom the number of tumor recurrences could not be determined, 42 patients (50%) had a single recurrent tumor, and 42 patients (50%) had multiple tumor recurrences (13 with 2 tumors and 29 with ≥ 3 tumors) (Fig.S2B). TTR was not significantly different between the IL-41 expression subgroups (Fig.S2C, D).

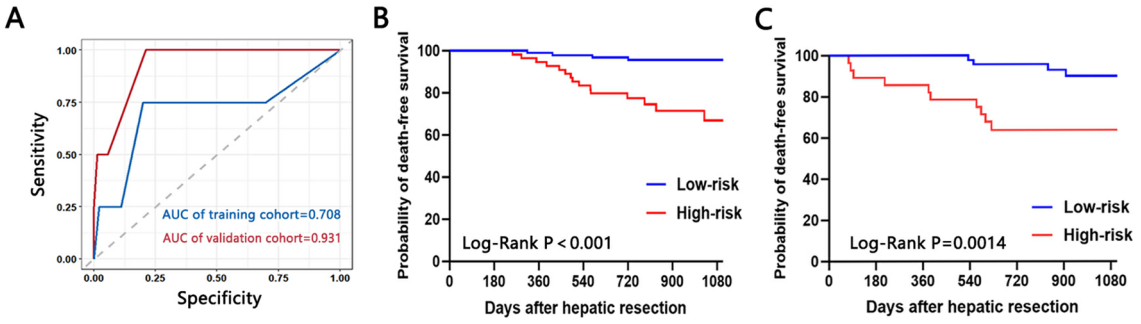

D

Months after Hepatic resection	0	6	12	18	24
No.of patients at risk					
Low-risk	93	93	92	90	81
High-risk	54	54	51	44	33

E

Months after Hepatic resection	0	6	12	18	24
No.of patients at risk					
Low-risk	46	46	46	45	38
High-risk	27	24	23	21	13

Fig. 6 Validation of the nomogram model for predicting death. **(A)** The ROC curve and AUC with 95% CI in the training cohort and validation cohort. Kaplan–Meier survival analysis of the high-risk, middle-risk, and low-risk HCC patients in the training cohort **(B)** and validation cohort **(C)**.Survival status of of high-risk, medium risk, and low-risk HCC patients in the training cohort **(D)** and validation cohort **(E)**. ROC, Receiver Operating Characteristic; AUC, Area Under Curve; CI, confidence interval

Univariate and multivariate analyses of adverse prognostic factors

The results of univariate and multivariate Cox proportional hazards regressions of RFS risk factors are presented in Table 2. Univariate analysis identified high IL-41 expression, intratumoral artery, MVI grade M1, and MVI grade M2 as potential predictive factors of recurrence following hepatectomy. Furthermore, multivariate Cox analysis indicated that high IL-41 expression ($P = 0.000$), intratumoral artery ($P = 0.005$), and MVI grade M1 ($P = 0.031$) were independent risk factors for recurrence following hepatectomy.

The results of univariate and multivariate Cox proportional risk regressions of PFS risk factors are summarized in Table 3. Univariate analysis identified high IL-41 expression, AFP positivity, irregular tumor shape, tumor size ≥ 5 cm, MVI grade M2, AST concentration of 45–90 pg/mL, a neutrophil count of $\leq 6.3 \times 10^9$/cell, and a lymphocyte count of $< 1.1 \times 10^9$/cell were potential predictors of post-hepatectomy mortality. Additionally, multivariate Cox analysis demonstrated that high IL-41 expression ($P = 0.000$), tumor size ≥ 5 cm ($P = 0.001$), and AST concentration 45–90 pg/mL ($P = 0.015$) were independent risk factors for post-hepatectomy mortality.

Forest plots were constructed to illustrate the effect of different risk factors on RFS and PFS in the training cohort (Tables 4 and 5)(Supplementary Fig. 1). The M2 grade and tumor size ≥ 5 cm were the strongest predictors of recurrence (hazard ratio [HR]: 3.824; 95% CI: 1.964, 7.445) and mortality (HR: 5.793; 95% CI: 2.148, 15.628).

Nomogram development and validation

A nomogram was developed to predict RFS at 12 and 36 months following radical hepatectomy in patients with HCC, utilizing significant risk factors identified through Cox regression analysis. Each regression coefficient was proportionally transformed into a scoring system ranging from 0 to 100, with the variable exhibiting the highest absolute β coefficient receiving a score of 100. M2 scored the highest (100), followed by high IL-41 expression (63.535), M1 (27.218), and intratumoral artery (23.490) (Fig.S3A, B).

To evaluate and compare the discriminative power of the nomogram in predicting the risk of post-hepatectomy recurrence, we calculated the AUCs of the model for the training and validation cohorts, which were 0.747 and 0.614, respectively (Figure S4A). Risk scores were calculated for each patient based on the developed nomogram, and an optimal cutoff of 38.963 was determined using the

Table 1 Demographic, clinical, pathological and imaging characteristics of HCC patients in the training and validation cohorts

Variables	Overall cohort (*n* = 224)	Training cohort (*n* = 149)	Validation cohort (*n* = 75)	*P*-Value
Sex				0.440
Male	174(77.7)	118(79.2)	56(74.7)	
Female	50(22.3)	31(20.8)	19(25.3)	
Age (years)				0.261
≥ 65	55(24.6)	40(26.8)	15(20.0)	
<65	169(75.4)	109(63.2)	60(80.0)	
HBV				0.071
Absent	143(63.8)	89(59.7)	54(72.0)	
Present	81(36.2)	60(40.3)	21(28.0)	
HCV				0.844
Absent	16(7.1)	11(7.4)	5(6.7)	
Present	208(92.9)	138(92.6)	70(93.3)	
Differentiation				0.524
Poor	33(14.7)	24(16.1)	9(12.0)	
Moderate	180(80.4)	119(79.9)	61(81.3)	
Well	11(4.9)	6(4.0)	5(6.7)	
AFP				0.421
AFP-Positive	116(51.8)	80(53.7)	36(48.0)	
AFP-Negative	108(48.2)	69(46.3)	39(52.0)	
IL41				0.203
IL41-High	112(50.0)	70(47.0)	42(56.0)	
IL41-Low	112(50.0)	79(53.0)	33(44.0)	
Narrow Surgical margin				0.685
Present	36(16.1)	25(16.8)	11(14.7)	
Absent	188(83.9)	124(83.2)	64(85.3)	
Intratumor hemorrhage				0.081
Present	6(2.7)	2(1.3)	4(5.3)	
Absent	218(97.3)	147(98.7)	71(94.7)	
Intratumoral artery				0.103
Present	54(24.1)	31(21)	23(30.7)	
Absent	170(75.9)	118(79.2)	52(69.3)	
Peritumoral enhancement				0.061
Present	31(13.8)	16(10.7)	15(20.0)	
Absent	192(86.2)	132(89.3)	60(80.0)	
Tumor shape				0.470
Regular shape	165(73.7)	112(75.2)	53(70.7)	
Irregular shape	59(26.3)	37(24.8)	22(29.3)	
Tumor size (cm)				0.571
≥ 5	75(33.5)	48(32.2)	27(36.0)	
<5	149(66.5)	101(67.8)	48(64.0)	
Multiple tumors				0.149
Absent	196(87.5)	127(85.2)	69(92.0)	
Present	28(22.5)	22(14.8)	6(8.0)	
MVI grade				0.555
M0	79(35.3)	55(36.9)	24(32.0)	
M1	86(38.4)	58(38.9)	28(37.3)	
M2	59(26.3)	36(24.2)	23(30.7)	
Satellite nodules				0.524
Present	34(15.2)	21(14.1)	13(17.3)	
Absent	190(84.8)	128(85.9)	62(82.7)	
Capsular invasion				0.464
Present	148(66.1)	96(64.4)	52(69.3)	

Table 1 (continued)

Variables	Overall cohort (*n* = 224)	Training cohort (*n* = 149)	Validation cohort (*n* = 75)	*P*-Value
Absent	76(33.9)	53(35.6)	23(30.7)	
Vascular invasion				0.503
Present	35(15.6)	25(16.8)	10(13.3)	
Absent	189(84.4)	124(83.2)	65(86.7)	
AST (U/L)				0.204
≤ 45	186(83.0)	119(79.9)	67(89.3)	
45–90	28(12.5)	22(14.8)	6(8.0)	
>90	10(4.5)	8(5.4)	2(2.7)	
ALT (U/L)				0.345
≤ 40	137(61.2)	87(58.4)	50(66.7)	
40–80	64(28.6)	44(29.5)	20(26.7)	
>80	23(10.3)	18(12.1)	5(6.6)	
Total bilirubin (umol/L)				0.160
≤ 17.1	141(62.9)	89(59.7)	52(69.3)	
>17.1	83(37.1)	60(40.3)	23(30.7)	
Direct bilirubin (umol/L)				0.948
≤ 3.4	77(34.4)	51(34.2)	26(34.7)	
>3.4	147(65.6)	98(65.8)	49(65.3)	
Serum albumin (g/L)				0.470
≥ 40	59(26.3)	37(24.8)	22(29.3)	
<40	165(73.7)	112(75.2)	53(70.7)	
Neutrophils (109/L)				0.990
>6.3	15(6.7)	10(6.7)	5(6.7)	
≤ 6.3	209(93.3)	139(93.3)	70(93.3)	
Platelet (109/L)				0.469
≥ 125	130(58.0)	89(59.7)	41(54.7)	
<125	94(42.0)	60(40.3)	34(35.3)	
Lymphocyte (109/L)				0.894
≥ 1.1	151(67.4)	100(67.1)	51(68.0)	
<1.1	73(32.6)	49(33.9)	24(32.0)	

Youden's index to stratify patients into the high-risk and low-risk groups. Kaplan-Meier survival analysis demonstrated that the 3-year RFS rate was significantly lower in the high-risk group (22.22%) than in the low-risk group (53.29%, $P < 0.001$; Fig.S4B). The same findings were also obtained for the validation cohort ($P = 0.0126$, Fig.S4C).

For the recurrence-free survival(RFS) nomogram, the C-index values were 0.692 in the training cohort and 0.688 in the validation cohort. Regarding the overall survival (OS) nomogram, the C-index values reached 0.781 in the training cohort and 0.796 in the validation cohort. Furthermore, the calibration curves demonstrated good agreement between the observed and predicted probabilities for 1-year and 3-year RFS (Supplementary Fig. 2A-D) and OS (Supplementary Fig. 2E-H) in both cohorts.

The same methods were employed to construct the nomogram for predicting PFS at 12 and 36 months after radical hepatectomy. Tumor size ≥ 5 cm had the highest score (100), followed by AST 40–90 pg/mL (86.170), AST > 90 pg/mL (81.275), and high IL-41 expression (69.638) (Fig.S3C, D). The AUC of this nomogram was 0.708 for the training cohort and 0.931 for the validation cohort (Fig.S6A). The optimal risk score cutoff was determined to be 93.085 using the Youden's index. Kaplan-Meier survival analysis demonstrated that the 3-year PFS rate was significantly higher in the low-risk group (30.86%) than in the high-risk group (6.99%, $P < 0.001$; Fig.S6B). Similar findings were obtained for the validation cohort ($P = 0.0014$, Fig.S6C). DCA indicated that using an risk score plot to predict recurrence (Fig.S5A, B) and mortality (Fig.S7A, B) may offer greater benefits compared to treating all patients in the training and validation cohorts or leaving them untreated. Consistent with this, CIC revealed that the nomogram had significantly higher predictive performance (Fig.S5C, D and Fig.S7C, D).

Discussion

Tumor recurrence and mortality are significant adverse prognoses for patients with HCC. In this retrospective study, IL-41, MVI, and intratumoral artery were

Table 2 Cox proportional hazards regression analysis of risk factors for early recurrence

Variables		Univariate analysis		Multivariate analysis	
		HR(95%CI)	*P*-Value	HR(95%CI)	*P*-Value
Sex	Male vs. Female	1.057(0.645,1.733)	0.825		
Age (years)	<65vs ≥ 65	1.284(0.784,2.104)	0.320		
HBV	None vs. HBV	1.081(0.705,1.660)	0.720		
HCV	None vs. HCV	1.233(0.539,2.821)	0.619		
Differentiation	Well		0.332		
	Poor vs. Well	2.729(0.627,11.878)	0.099		
	Moderate vs. Well	2.077(0.508, 8.493)	0.157		
AFP	AFP-Negative vs. AFP-Positive	0.902(0.738,1.101)	0.311		
IL41	IL41-High vs. IL41-Low	2.312(1.528,3.498)	**0.000**	2.446(1.528,3.498)	**0.000**
Intratumor necrosis	Absent vs. Present	0.663(0.397,1.109)	0.117		
Intratumor hemorrhage	Absent vs. Present	20.936(0.075,5834.267)	0.290		
Intratumoral artery	Present vs. Absent	1.945(1.271,2.985)	**0.002**	1.862(1.160,2.882)	**0.005**
Peritumoral enhancement	Absent vs. Present	0.750(0.438,1.286)	0.296		
Tumor shape	Regular shape vs. Irregular shape	0.910(0.582,1.424)	0.680		
Tumor size (cm)	<5 vs. ≥ 5	0.681(0.452,1.027)	0.067	0.751(0.482,1.169)	0.205
Multiple tumors	Absent vs. Present	0.849(0.463,1.555)	0.596		
MVI grade	MV0		**0.006**		**0.049**
	MV1 vs. MV0	2.311(1.370,3.900)	**0.002**	1.541(0.962,2.470)	**0.031**
	MV2 vs. MV0	1.458(0.881,2.413)	0.052	1.838(1.059,3.185)	0.072
Satellite nodules	Absent vs. Present	1.049(0.600,1.835)	0.866		
Capsular invasion	Absent vs. Present	0.851(0.553,1.310)	0.464		
Narrow Surgical margin	Absent vs. Present	0.788(0.527,1.179)	0.247		
Vascular invasion	Absent vs. Present	0.972(0.567,1.667)	0.918		
AST (U/L)	≤ 45		0.836		
	45<≤90vs ≤ 45	0.774(0.313,1.914)	0.578		
	>90vs ≤ 45	0.730(0.251,2.128)	0.564		
ALT (U/L)	≤ 40		0.436		
	40<≤80vs ≤ 40	0.923(0.472,1.806)	0.816		
	>80vs ≤ 40	0.692(0.330,1.450)	0.330		
Total bilirubin (umol/L)	≤ 17.1vs >17.1	1.045(0.690,1.583)	0.835		
Direct bilirubin (umol/L)	≤ 3.4vs>3.4	1.216(0.806,1.834)	0.351		
Serum albumin (g/L)	<40vs ≥ 40	0.937(0.600,1.462)	0.774		
Neutrophils (109/L)	≤ 6.3vs>6.3	0.842(0.382,1.858)	0.671		
Platelet (109/L)	<125vs ≥ 125	0.947(0.630,1.423)	0.793		
Lymphocyte (109/L)	<1.1vs ≥ 1.1	1.114(0.729,1.703)	0.617		

identified as independent risk factors for post-hepatectomy recurrence, while IL-41, tumor size, and AST levels were independent risk factors for post-hepatectomy mortality. By integrating these risk factors, two multivariate nomograms were developed and validated to predict the 12- and 36-month RFS and PFS of HCC patients, respectively. The findings demonstrated that IL-41 was an important marker for predicting postoperative HCC recurrence and mortality, highlighting its potential as a prognostic factor for HCC. Although IL-41 replaced the predictive role of AFP in this study, this does not imply that AFP is no longer a useful tool for assessing HCC prognosis. This may be attributed to the high proportion of AFP-negative patients included in the study. Nonetheless, these results highlight the significance of post-resection recurrence and mortality in AFP-negative HCC patients, where the lack of a significantly elevated serum AFP level underscores the critical role of IL-41 in predicting prognosis.

The prognostic value of MVI in HCC was first demonstrated at the 2013 International Consensus Conference on Hepatocellular Carcinoma and Liver Transplantation. Since then, MVI is considered a key factor in the early recurrence and poor prognosis of HCC [31]. The dissemination of malignant cells via the vasculature represents a critical mechanism driving early recurrence [32]. Angiogenesis is a common defining characteristic among HCC and other cancers. MVI occurs when HCC cells acquire the ability to invade the vasculature, enabling metastasis [33]. Consistent with previous findings, we demonstrated that intratumoral arteries are an independent risk factor for recurrence [34]. Additionally, intratumoral

Table 3 Cox proportional hazards regression analysis of risk factors for death

Variables		Univariate analysis		Multivariate analysis	
		HR(95%CI)	*P*-Value	HR(95%CI)	*P*-Value
Sex	Male vs. Female	1.057(0.353,1.545)	0.738		
Age (years)	<65vs ≥ 65	0.588(0.291,1.189)	0.140		
HBV	None vs. HBV	1.319(0.653,2.665)	0.441		
HCV	None vs. HCV	0.738(0.226,2.415)	0.615		
Differentiation	Well		0.842		
	Poor vs. Well	1.879(0.219,16.096)	0.565		
	Moderate vs. Well	1.774(0.241, 13.055)	0.573		
AFP	AFP-Negative vs. AFP-Positive	0.390(0.187,0.813)	**0.012**	0.563(0.258,1.225)	0.147
IL−41	IL−41-High vs. IL−41-Low	2.967(1.420,6.198)	**0.004**	4.679(2.087,10.488)	**0.000**
Intratumor necrosis	Absent vs. Present	0.660(0.287,1.517)	0.328		
Intratumor hemorrhage	Absent vs. Present	0.333(0.080,1.392)	0.132		
Intratumoral artery	Absent vs. Present	0.617(0.301,1.268)	0.189		
Peritumoral enhancement	Absent vs. Present	1.726(0.527,5.657)	0.368		
Tumor shape	Regular shape vs. Irregular shape	0.424(0.215,0.835)	**0.016**	0.628(0.304,1.296)	0.208
Tumor size (cm)	≥ 5vs<5	5.155(2.506,10.616)	**0.000**	3.745(1.684,8.334)	**0.001**
Multiple tumors	Absent vs. Present	0.493(0.215,1.133)	0.096		
MVI grade	MV0		**0.004**		0.166
	MV1 vs. MV0	1.169(0.461,2.963)	0.743	0.741(0.275,2.001)	0.555
	MV2 vs. MV0	3.367(1.441,7.868)	**0.005**	1.615(0.629,4.142)	0.319
Satellite nodules	Absent vs. Present	1.027(0.398,2.655)	0.955		
Capsular invasion	Absent vs. Present	0.474(0.207,1.090)	0.079		
Narrow Surgical margin	Absent vs. Present	1.091(0.557,2.137)	0.799		
Vascular invasion	Absent vs. Present	0.571(0.258,1.262)	0.166		
AST (U/L)	≤ 45		**0.001**		**0.048**
	45<≤90vs ≤ 45	4.050(1.906,8.608)	**0.000**	2.837(1.223,6.580)	**0.015**
	>90vs ≤ 45	2.291(0.627,8.367)	0.210	1.887(0.505,7.047)	0.345
ALT (U/L)	≤ 40		0.100		
	40<≤80vs ≤ 40	0.528(0.215,1.299)	0.164		
	>80vs ≤ 40	1.844(0.745,4.566)	0.186		
Total bilirubin (umol/L)	≤ 17.1vs >17.1	0.715(0.363,1.407)	0.331		
Direct bilirubin (umol/L)	≤ 3.4vs>3.4	0.517(0.225,1.189)	0.120		
Serum albumin (g/L)	<40vs ≥ 40	2.827(0.996,8.027)	0.051		
Neutrophils (109/L)	≤ 6.3vs>6.3	0.282(0.116,0.684)	**0.005**	0.499(0.167,1.494)	0.214
Platelet (109/L)	<125vs ≥ 125	0.585(0.286,1.196)	0.142		
Lymphocyte (109/L)	<1.1vs ≥ 1.1	2.284(1.166,4.475)	**0.016**	1.939(0.910,4.131)	0.086

Table 4 The forest plot of multivariate Cox regression analysis of recurrence risk factors

	No.of patients	β coefficient	*P* value	HR(95%CI)
MVI grade: M1	58	0.365	0.270	1.441(0.753,2.755)
MVI grade: M2	36	1.341	**0.000**	3.824(1.964,7.445)
Intratumoral artery	31	0.315	0.281	1.370(0.773,2.427)
High expression of IL−41	70	0.852	**0.001**	2.345(1.409,3.906)

Table 5 The forest plot of multivariate Cox regression analysis of death risk factors

	No.of patients	β coefficient	*P* value	HR(95%CI)
AST:>90pg/ml	8	1.428	0.069	4.170(0.893,19.467)
AST:40−90pg/ml	22	1.514	**0.003**	4.545(1.696,12.180)
Tumor size:>5 cm	48	1.757	**0.001**	5.793(2.148,15.628)
High expression of IL−41	70	1.213	**0.013**	3.365(1.295,8.740)

arteriogenesis was strongly associated with MVI [35, 36], suggesting a potential link between factors affecting tumor prognosis (see Fig. 7).

Tumor size is a significant predictor of prognosis in HCC patients who have undergone R0 resection [38], as

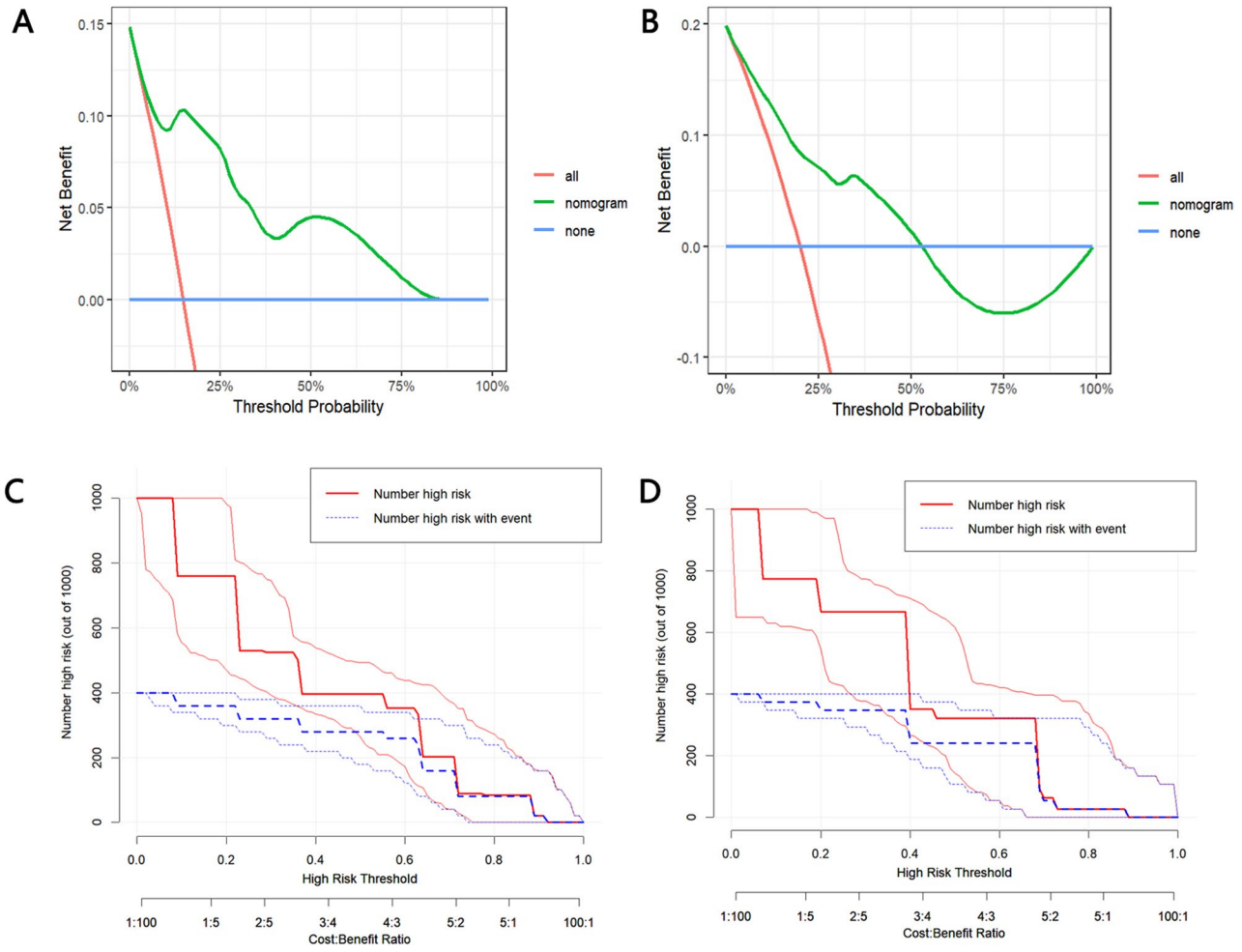

Fig. 7 DCA of column charts in training and validation cohort **(A**, **B)**. The Y-axis displays net benefits. The X-axis represents the threshold probability. None-line (blue line) represents the net benefit when no participant is considered dead. All-line(red line) represents the net benefit when all participants are considered dead. The green line represents the net benefit of the nomogram at different threshold probabilities. The area between the "none-line" (blue line) and "all-line" (red line) in the model curve represents the clinical practicality of the model. CIC for predicting the presence of death in the column chart of the training cohort **(C)** and validation cohort **(D)**. Under different threshold probabilities in a given population, the number of high-risk patients and the number of high-risk patients who died are displayed.DCA, Decision Curve Analysis; CIC, Clinical impact curve

larger tumors are often associated with adverse prognostic factors such as MVI and poorer postoperative outcomes [37, 39, 40].

AST is a liver enzyme released by hepatocytes upon damage [37]. Studies have demonstrated that elevated AST levels are significantly associated with liver diseases such as alcoholic hepatitis, hepatitis B, and HCC, and are a prognostic factor for poor postoperative outcomes in HCC patients. Consistent with its important role in assessing liver function and liver disease outcomes, we found that AST is a significant independent risk factor for predicting postoperative mortality in HCC, suggesting a close relationship between liver function and mortality in these patients.

Current evidence indicates that liver inflammation is a strong predictor of poor postoperative prognosis in HCC [41]. IL-41 is markedly elevated in a number of inflammatory conditions, including inflammatory bowel disease, sepsis, and psoriatic arthritis. IL-41 has been demonstrated to promote tissue repair [42–44], and its high expression can be influenced by inflammation [45]. Consequently, IL-41 may represent a potential therapeutic target and diagnostic marker for a wide range of immune diseases, and its role in postoperative HCC outcomes merits further investigation. Elevated tissue IL-41 expression was previously observed in HCC patients who experienced early recurrence and mortality following resection. In line with this, the present study also indicated that patients with high IL-41 expression exhibited significantly reduced RFS and PFS compared to patients with low IL-41 expression. Consequently, IL-41 was incorporated as a predictor of HCC recurrence and mortality after R0 resection into the current prediction model.

The developed nomograms demonstrated satisfactory performance in predicting postoperative recurrence (AUCs: 0.747 for training cohort, 0.614 for validation cohort) and mortality (AUCs: 0.708 for training cohort and 0.931 validation cohort). A key advantage of this nomogram is that all the risk factors incorporated into the model can be readily obtained through standard serological and imaging tests, thereby making the model suitable for clinical application. Nevertheless, several limitations should be taken into consideration. This was a single-center retrospective study, which may be prone to selection bias. Additionally, the prediction model was not externally validated using samples from other centers or sources. The independent risk factors for recurrence and mortality were identified using data from the entire study population, in contrast to Cox regression analyses that were limited to the training cohort alone. The former allows for a more comprehensive identification of independent risk factors across a larger sample, whereas the latter may lead to the identification of factors that are not truly independent. The independent risk factors identified in this manner may not be associated with the occurrence of events in the training cohort, resulting in some margin of error.

In conclusion, IL-41, MVI, and intratumoral artery are independent risk factors for post-hepatectomy recurrence, while IL-41, tumor size, and AST are independent risk factors for post-hepatectomy mortality in HCC. The two multivariate nomograms developed using these risk factors demonstrated satisfactory performance in predicting HCC recurrence and mortality at 12 and 36 months after R0 resection.

Abbreviations

HCC	Hepatocellular carcinoma
IL-41	Interleukin-41
MVI	Microvascular invasion
ALT	Alanine transaminase
AST	Aspartate transaminase
AFP	Alpha-fetoprotein
HBV	Hepatitis B virus
HCV	Hepatitis C virus
OS	Overall survival
RFS	Recurrence-free survival
PFS	Progression-free survival
TTR	Time to disease recurrence
ELISA	Enzyme-linked immunosorbent assay
CNLC	Chinese Liver Cancer Stage
PVTT	Portal vein tumor thrombus
Streptavidin-HRP	Horseradish peroxidase-labeled streptavidin
CT	Computed Tomography
MRI	Magnetic Resonance Imaging
OD	Optical Density
ROC	Receiver Operating Characteristic
AUC	Area Under Curve
DCA	Decision Curve Analysis
CIC	Clinical impact curve
NLR	Neutrophil-to-lymphocyte ratio
PLR	Platelet-to-lymphocyte ratio
CNP	C-type natriuretic peptide
IL-6	Interleukin-6
DCP	Des-γ-carboxy prothrombin
AFP-L3	α-fetoprotein-L3

Supplementary Information

The online version contains supplementary material available at https://doi.org/10.1186/s12885-025-14344-0.

Supplementary Material 1: Supplementary Fig. 1: The forest plot of multivariate Cox regression analysis. (A) The forest plot of multivariate Cox regression analysis of recurrence risk factors. IL41,interleukin-41;MVI, microvascular invasion; HR, hazard ratio. (B)The forest plot of multivariate Cox regression analysis of death risk factors. AFP, alpha fetoprotein; IL41,interleukin-41; AST, aspartate transaminase; HR, hazard ratio

Supplementary Material 2: Supplementary Fig. 2: Calibration curves of nomograms for predicting 1-year and 3-year recurrence free survival (RFS) and overall survival (OS). (A) 1-year RFS in training cohort. (B) 1-year RFS in validation cohort. (C) 3-year RFS in training cohort. (D) 3-year RFS in validation cohort. (E) 1-year OS in training cohort. (F) 1-year OS in validation cohort. (G) 3-year OS in training cohort. (H) 3-year OS in validation cohort. RFS: recurrence-free survival; OS: overall survival

Acknowledgements
All data in this retrospective study were obtained from the electronic medical record system of the First Affiliated Hospital of Xi'an Jiaotong University.

Author contributions
YB conceived and designed this study. YB and LY supervised the study. YB and LY obtained the research funding. YB, SJ, and MZ performed the statistical analysis. MZ and YB performed the data processing and analysis. MZ drafted the manuscript. SJ, YJiu, FR, and YJia assisted in drafting the manuscript. YB reviewed and revised the manuscript. All authors contributed to the manuscript and approved the submitted version.

Funding
The author(s) declare financial support was received for the research, authorship, and/or publication of this article. This study was supported by Hospital Research and Development Fund of the First Affiliated Hospital of Xi'an Jiaotong University (2021QN-04), Research and Development Program Fund of Shaanxi Province (2023-JC-YB-680), National Natural Science Foundation of China (82303460), Hospital Research and Development Fund of the First Affiliated Hospital of Xi'an Jiaotong University (2022QN-30), Research and Development Program Fund of Shaanxi Province(2024JC-YBQN-0897).

Data availability
The studies involving humans were approved by the Ethics Committee of Xi'an Jiaotong University. The studies were conducted in accordance with the local legislation and institutional requirements. Written informed consent for participation in this study was provided by the participants' legal guardians/next ofkin. Written informed consent was obtained from the individual(s) for the publication of any potentially identifiable images or data included in this article.

Declarations

Ethics approval and consent to participate
The studies involving humans were approved by the Ethics Committee of Xi'an Jiaotong University. The studies were conducted in accordance with the local legislation and institutional requirements. Written informed consent for participation in this study was provided by the participants' legal guardians/next of kin. Written informed consent was obtained from the individual(s) for the publication of any potentially identifiable images or data included in this article.

Consent for publication
Not applicable.

Approval committee
Xi'an Jiaotong University.

Competing interests
The authors declare no competing interests.

Received: 28 March 2025 / Accepted: 16 May 2025
Published online: 26 May 2025

References

1. Bray F, Laversanne M, Sung H, et al. Global cancer statistics 2022: GLOBOCAN estimates of incidence and mortality worldwide for 36 cancers in 185 countries. CA Cancer J Clin. 2024;74(3):229–63. https://doi.org/10.3322/caac.21834.
2. Xie D, Shi J, Zhou J, Fan J, Gao Q. Clinical practice guidelines and real-life practice in hepatocellular carcinoma: A Chinese perspective. Clin Mol Hepatol. 2023;29(2):206–16. https://doi.org/10.3350/cmh.2022.0402.
3. Roayaie S, Obeidat K, Sposito C, et al. Resection of hepatocellular cancer ≤ 2 cm: results from two Western centers. Hepatology. 2013;57(4):1426–35. https://doi.org/10.1002/hep.25832.
4. Moriguchi M, Takayama T, Higaki T, et al. Early cancer-related death after resection of hepatocellular carcinoma. Surgery. 2012;151(2):232–7. https://doi.org/10.1016/j.surg.2010.10.017.
5. Simsek C, Kim A, Ma M, et al. Recurrence of hepatocellular carcinoma following deceased donor liver transplantation: case series. Hepatoma Res. 2020;6:11. https://doi.org/10.20517/2394-5079.2019.51.
6. Tabrizian P, Jibara G, Shrager B, Schwartz M, Roayaie S. Recurrence of hepatocellular cancer after resection: patterns, treatments, and prognosis. Ann Surg. 2015;261(5):947–55. https://doi.org/10.1097/SLA.0000000000000710.
7. Jung SW, Kim DS, Yu YD, Han JH, Suh SO. Risk factors for cancer recurrence or death within 6 months after liver resection in patients with colorectal cancer liver metastasis. Ann Surg Treat Res. 2016;90(5):257–64. https://doi.org/10.4174/astr.2016.90.5.257.
8. Xu XF, Xing H, Han J, et al. Risk factors, patterns, and outcomes of late recurrence after liver resection for hepatocellular carcinoma: A multicenter study from China. JAMA Surg. 2019;154(3):209–17. https://doi.org/10.1001/jamasurg.2018.4334.
9. Lim KC, Chow PK, Allen JC, et al. Microvascular invasion is a better predictor of tumor recurrence and overall survival following surgical resection for hepatocellular carcinoma compared to the Milan criteria. Ann Surg. 2011;254(1):108–13. https://doi.org/10.1097/SLA.0b013e31821ad884.
10. Shah PA, Patil R, Harrison SA. NAFLD-related hepatocellular carcinoma: the growing challenge. Hepatology. 2023;77(1):323–38. https://doi.org/10.1002/hep.32542.
11. He Z, She X, Liu Z, et al. Advances in post-operative prognostic models for hepatocellular carcinoma. J Zhejiang Univ Sci B. 2023;24(3):191–206. https://doi.org/10.1631/jzus.B2200067.
12. Gao XX, Li JF. Current strategies for predicting post-hepatectomy liver failure and a new ultrasound-based nomogram. World J Gastroenterol. 2024;30(39):4254–9. https://doi.org/10.3748/wjg.v30.i39.4254.
13. Harding-Theobald E, Louissaint J, Maraj B, et al. Systematic review: radiomics for the diagnosis and prognosis of hepatocellular carcinoma. Aliment Pharmacol Ther. 2021;54(7):890–901. https://doi.org/10.1111/apt.16563.
14. Ji GW, Zhu FP, Xu Q, et al. Machine-learning analysis of contrast-enhanced CT radiomics predicts recurrence of hepatocellular carcinoma after resection: A multi-institutional study. EBioMedicine. 2019;50:156–65. https://doi.org/10.1016/j.ebiom.2019.10.057.
15. Regimbeau JM, Abdalla EK, Vauthey JN, et al. Risk factors for early death due to recurrence after liver resection for hepatocellular carcinoma: results of a multicenter study. J Surg Oncol. 2004;85(1):36–41. https://doi.org/10.1002/jso.10284.
16. Yan M, Zhang X, Zhang B, et al. Deep learning nomogram based on Gd-EOB-DTPA MRI for predicting early recurrence in hepatocellular carcinoma after hepatectomy. Eur Radiol. 2023;33(7):4949–61. https://doi.org/10.1007/s00330-023-09419-0.
17. Wu Z, Tang H, Wang L et al. Postoperative survival analysis of hepatocellular carcinoma patients with liver cirrhosis based on propensity score matching. BMC Surg. 2022;22(1):103. Published 2022 Mar 21. https://doi.org/10.1186/s12893-022-01556-5
18. Xiong SP, Wang CH, Zhang MF, Yang X, Yun JP, Liu LL. A multi-parametric prognostic model based on clinicopathologic features: vessels encapsulating tumor clusters and hepatic plates predict overall survival in hepatocellular carcinoma patients. J Transl Med. 2024;22(1):472. Published 2024 May 18. https://doi.org/10.1186/s12967-024-05296-3
19. Shen D, Sha L, Yang L, Gu X. Based on disulfidptosis, unveiling the prognostic and immunological signatures of Asian hepatocellular carcinoma and identifying the potential therapeutic target ZNF337-AS1. Discov Oncol. 2025;16(1):544. Published 2025 Apr 17. https://doi.org/10.1007/s12672-025-02325-5
20. Rocco A, Sgamato C, Pelizzaro F, et al. Systemic inflammatory response markers improve the discrimination for prognostic model in hepatocellular carcinoma. Hepatol Int Published Online March. 2025;25. https://doi.org/10.1007/s12072-025-10806-6.
21. Wu DH, Liao CY, Wang DF, et al. Textbook outcomes of hepatocellular carcinoma patients with sarcopenia: A multicenter analysis. Eur J Surg Oncol. 2023;49(4):802–10. https://doi.org/10.1016/j.ejso.2022.12.009.
22. Xu J, Lin H, Wu G, Zhu M, Li M. IL-6/STAT3 is a promising therapeutic target for hepatocellular carcinoma. Front Oncol. 2021;11:760971. https://doi.org/10.3389/fonc.2021.760971. Published 2021 Dec 15.
23. Norman JS, Li PJ, Kotwani P, Shui AM, Yao F, Mehta N. AFP-L3 and DCP strongly predict early hepatocellular carcinoma recurrence after liver transplantation. J Hepatol. 2023;79(6):1469–77. https://doi.org/10.1016/j.jhep.2023.08.020.
24. Li Y, Wang H, Ren D et al. Interleukin-41: a novel serum marker for the diagnosis of alpha-fetoprotein-negative hepatocellular carcinoma. Front Oncol. 2024;14:1408584. Published 2024 May 21. https://doi.org/10.3389/fonc.2024.1408584
25. Tan XP, Zhou K, Zeng QL, Yuan YF, Chen W. Influence of AFP on surgical outcomes in non-B non-C patients with curative resection for hepatocellular carcinoma. Clin Exp Med. 2023;23(1):107–15. https://doi.org/10.1007/s10238-022-00813-4.
26. Huang J, Liu FC, Li L, Zhou WP, Jiang BG, Pan ZY. Nomograms to predict the long-time prognosis in patients with alpha-fetoprotein negative hepatocellular carcinoma following radical resection. Cancer Med. 2020;9(8):2791–802. https://doi.org/10.1002/cam4.2944.
27. Zhou D, Liu X, Wang X et al. A prognostic nomogram based on LASSO Cox regression in patients with alpha-fetoprotein-negative hepatocellular carcinoma following non-surgical therapy. BMC Cancer. 2021;21(1):246. Published 2021 Mar 8. https://doi.org/10.1186/s12885-021-07916-3
28. Thokerunga E, Kisembo P, FangFang H, et al. Serum midkine for AFP-negative hepatocellular carcinoma diagnosis: a systematic review and meta-analysis. Egypt Liver J. 2023;13:25. https://doi.org/10.1186/s43066-023-00259-7.
29. Asif HM, Zafar F, Ahmad K et al. Synthesis, characterization and evaluation of anti-arthritic and anti-inflammatory potential of curcumin loaded chitosan nanoparticles. Sci Rep. 2023;13(1):10274. Published 2023 Jun 24. https://doi.org/10.1038/s41598-023-37152-7
30. Liu K, Ding Y, Wang Y, et al. Combination of IL-34 and AFP improves the diagnostic value during the development of HBV related hepatocellular carcinoma. Clin Exp Med. 2023;23(2):397–409. https://doi.org/10.1007/s10238-022-00810-7.
31. Li K, Zhang R, Wen F, et al. Single-cell dissection of the multicellular ecosystem and molecular features underlying microvascular invasion in HCC. Hepatology. 2024;79(6):1293–309. https://doi.org/10.1097/HEP.0000000000000673.
32. Sumie S, Kuromatsu R, Okuda K, et al. Microvascular invasion in patients with hepatocellular carcinoma and its predictable clinicopathological factors. Ann Surg Oncol. 2008;15(5):1375–82. https://doi.org/10.1245/s10434-008-9846-9.
33. Rodríguez-Perálvarez M, Luong TV, Andreana L, Meyer T, Dhillon AP, Burroughs AK. A systematic review of microvascular invasion in hepatocellular carcinoma: diagnostic and prognostic variability. Ann Surg Oncol. 2013;20(1):325–39. https://doi.org/10.1245/s10434-012-2513-1.
34. Jiang H, Qin Y, Wei H, et al. Prognostic MRI features to predict postresection survivals for very early to intermediate stage hepatocellular carcinoma. Eur Radiol. 2024;34(5):3163–82. https://doi.org/10.1007/s00330-023-10279-x.
35. Jiang H, Wei J, Fu F, et al. Predicting microvascular invasion in hepatocellular carcinoma: A dual-institution study on gadoxetate disodium-enhanced MRI. Liver Int. 2022;42(5):1158–72. https://doi.org/10.1111/liv.15231.
36. Huo RR, Pan LX, Wu PS, et al. Prognostic value of aspartate aminotransferase/alanine aminotransferase ratio in hepatocellular carcinoma after hepatectomy. BJS Open. 2024;8(1):zrad155. https://doi.org/10.1093/bjsopen/zrad155.
37. Oh RC, Hustead TR, Ali SM, Pantsari MW. Mildly elevated liver transaminase levels: causes and evaluation. Am Fam Physician. 2017;96(11):709–15.
38. Huang WJ, Jeng YM, Lai HS, Sheu FY, Lai PL, Yuan RH. Tumor size is a major determinant of prognosis of resected stage I hepatocellular carcinoma. Langenbecks Arch Surg. 2015;400(6):725–34. https://doi.org/10.1007/s00423-015-1329-4.

39. Jonas S, Bechstein WO, Steinmüller T, et al. Vascular invasion and histopathologic grading determine outcome after liver transplantation for hepatocellular carcinoma in cirrhosis. Hepatology. 2001;33(5):1080–6. https://doi.org/10.1053/jhep.2001.23561.
40. Shehta A, Elsabbagh AM, Medhat M et al. Impact of tumor size on the outcomes of hepatic resection for hepatocellular carcinoma: a retrospective study. BMC Surg. 2024;24(1):7. Published 2024 Jan 3. https://doi.org/10.1186/s12893-023-02296-w
41. Zhang SL, Li ZY, Wang DS, et al. Aggravated ulcerative colitis caused by intestinal Metrnl deficiency is associated with reduced autophagy in epithelial cells. Acta Pharmacol Sin. 2020;41(6):763–70. https://doi.org/10.1038/s41401-019-0343-4.
42. Ushach I, Arrevillaga-Boni G, Heller GN, et al. Meteorin-like/Meteorin-β is a novel immunoregulatory cytokine associated with inflammation. J Immunol. 2018;201(12):3669–76. https://doi.org/10.4049/jimmunol.1800435.
43. Chen S, Shen B, Wu Y, et al. The relationship between the efficacy of thermal ablation and inflammatory response and immune status in early hepatocellular carcinoma and the progress of postoperative adjuvant therapy. Int Immunopharmacol. 2023;119:110228. https://doi.org/10.1016/j.intimp.2023.110228.
44. Nishino J, Yamashita K, Hashiguchi H, Fujii H, Shimazaki T, Hamada H. Meteorin: a secreted protein that regulates glial cell differentiation and promotes axonal extension. EMBO J. 2004;23(9):1998–2008. https://doi.org/10.1038/sj.emboj.7600202.
45. Rao RR, Long JZ, White JP, et al. Meteorin-like is a hormone that regulates immune-adipose interactions to increase beige fat thermogenesis. Cell. 2014;157(6):1279–91. https://doi.org/10.1016/j.cell.2014.03.065.

Publisher's note